JOURNAL OF SOLID STATE CHEMISTRY 37, 370–382 (1981)

Structure Relationships Affecting the Stability of *A*15- and Ti_3P-Type Compounds

R. M. WATERSTRAT

American Dental Association Health Foundation Research Unit, National Bureau of Standards, Washington, D.C. 20234

Received July 28, 1980; in revised form October 28, 1980

Observed interatomic distances in *A*15- and Ti_3P-type compounds are analyzed as deformations of ideal atomic rigid spheres. The analysis suggests that structural instabilities may develop in *A*15 compounds when the atomic size of the *B* element becomes approximately 10% smaller than that of the *A* element. These instabilities apparently originate from strong repulsive interactions along the atom chains. The internal strains associated with these interactions may be relieved by martensitic transformations, deviations from the ideal A_3B stoichiometry, addition of ternary elements, and transformation to a Ti_3P-type structure. Instability apparently develops in the Ti_3P-type compounds when the *A*- and *B*-element atoms are nearly equal in size. The instability in this case would result primarily from repulsive forces associated with a strong compression of the *B*-element atoms.

Introduction

Interatomic distances in covalent compounds can often be related to the filling of electronic bonding orbitals using equations such as those developed by Pauling (*1*). Pauling has noted, however, that metallic compounds may have distances which represent bonds in tension or compression and, in such cases, the use of Pauling's equations may lead to errors (*2, 3*). The source of these errors is suggested by Pearson's analysis of the interatomic distances in metal compounds (*4*). Pearson shows that the geometry of metallic structures may limit or control the electronic interactions. Pearson analyzes the interatomic distances by introducing an atomic "strain" parameter which is directly related to the relative atomic sizes through the structure geometry (*4, 5*). A comparison of structure geometries may therefore assist in understanding the relative stability of competing structures when electronic bonding considerations or band-structure calculations may not provide sufficient insight.

For example, it is difficult to see why the filling of bonding orbitals would differ significantly in compounds such as Nb_3Ge and Nb_3Si, but Nb_3Ge crystallizes in an *A*15 structure while Nb_3Si crystallizes in a Ti_3P-type structure.[1] This fact, however, is explainable by atomic packing considerations since the size of a Si atom is significantly less than that of a Ge atom. It will be shown in this paper that this size difference is critical in these two structures as a result of geometrical relationships.

[1] It should be noted, however, that Nb–Si *A*15 structures can crystallize metastably over a range of nonstoichiometric (Nb-rich) compositions (*6*).

0022-4596/81/060370-13$02.00/0

Previous Studies

The dominant geometric feature of the cubic *A*15 structure is its array of linear, mutually orthogonal *A*-atom chains (see Fig. 1). Interspersed homogeneously between these chains is a body-centered cubic *B*-atom sublattice whose sites are usually occupied by a different chemical element than that which occupies the atom-chain sites.

A close relationship has been suggested between the *A*15- and Ti_3P-type structures based on the similarity of certain atom networks (*7*), but these similarities are observed in a majority of metal structures (*8*) and probably have no unusual significance except to reflect a common tendency for such structures to form densely packed atomic layers.

Lattice parameters for *A*15 compounds can be calculated rather accurately using a set of atomic radii developed by Geller (*9*), but the implicit assumption that the atom sizes are fixed and independent of the identity of their atom partners is contradicted by the observed behavior of the *A*–*A* distances (*10*). The success of this method in calculating lattice parameters arises mainly from the "ideal" behavior of the *A*–*B* distances rather than from the correctness of a "rigid-sphere" approximation.

A development of great interest to this topic is the recent electron density measurements by Staudenmann on the *A*15 compounds V_3Si and Cr_3Si. Staudenmann (*11, 12*) observes a pronounced maximum in electron density between V atoms in the atom-chain sites but a remarkable absence of such an effect between Cr atoms. Thus the strength of the electronic interactions does not seem to account for the unusually short distances in all cases. One may perhaps attribute the short distances partly to geometrical packing considerations. This would produce a compression of these distances as will be shown in this paper.

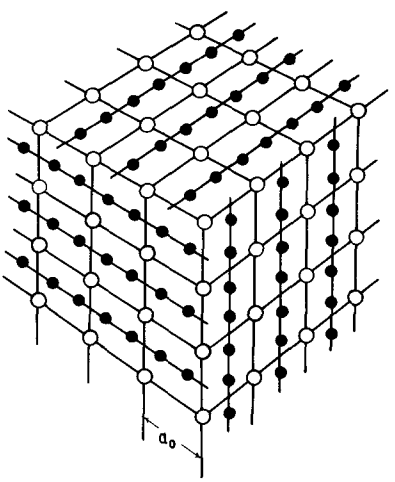

FIG. 1. Atomic structure of the *A*15 compounds (A_3B). *B* atoms located at the center of each cube are not visible in this projection. (●, *A* atoms; ○, *B* atoms.)

Experimental Procedures

The present study seeks to avoid the pitfalls of "rigid-sphere" models and preconceived notions about the "bonding" or structural "similarities." The emphasis is on models in which the atoms are regarded as being compressible objects which may change their size and shape in response to geometrical packing requirements so as to form spatial configurations which can extend infinitely in space as atoms must do in forming a macroscopic crystal. Rigid-sphere models are used only as a basis for exploring how the actual structures deviate from such a model and reasons are sought for these observed deviations. The probable existence of hybrid *s*, *p*, or *d* bonding orbitals is not discussed explicitly since this paper is mainly concerned with geometric effects, but bonding interactions among the various atomic orbitals will certainly occur to a varying extent among the different compounds. The bonding interactions may well be compatible with the geometric argu-

ments and should perhaps be considered in a future study.

The question of which atom pairs should be considered as "neighbors" could not be avoided since it was desirable to construct "coordination polyhedra" in order to compare the structures of *A*15 and Ti_3P compounds. Various definitions have been proposed in previous studies (*13–16*) and it is clear that the choice of definition must, to some extent, be arbitrary. Definitions yielding nonintegral numbers of neighbors are unsuitable since this would not permit construction of a polyhedron. The definition proposed by Frank and Kasper (*13*) was eventually adopted since it is unequivocal and yields only integral numbers. Other definitions might be chosen but the choice is not critical. The conclusions reached in this study generally do not depend on the definition of terms such as "neighbor" or "coordination number."

The atomic radii (and the corresponding atomic diameters D_A, D_B) used in this study were taken from the compilation of Teatum *et al.* appearing in Pearson's book (*17*), except for the radii of As and P atoms for which the values of Teatum *et al.* appear to be unsuitable in view of observed lattice parameter relationships in *A*15 compounds.[2] Therefore values of the atomic radii for As and P (1.355 and 1.230 Å, respectively) were obtained by interpolation and extrapolation using modified Nevitt-type plots (*10*) for observed *A*15 and Ti_3P compounds. These plots were constructed by substituting the observed atomic volumes (volume of the unit cell/number of atoms per unit cell) for the lattice parameter as the ordinate and substituting the *B*-element atomic volume (volume of a sphere having a diameter D_B) for the B-element atomic diameter as the abscissa. The use of observed atomic volumes rather than lattice parameters was necessary in order to accommodate the Ti_3P structure, which is tetragonal. The observed lattice parameters for the various phases were taken from the original sources wherever possible. In the case of *A*15 phases, however, the observed values were corrected for deviations from the ideal (A_3B) stoichiometry whenever such deviations were known to occur (see Table I). This was done by extrapolating the observed values in binary or ternary systems. In all cases, this correction was relatively small (<2%) and does not have a critical influence on the data. All distances are given in angstroms.

The atomic position parameters and tetragonal c/a ratio of the compound Nb_3Si (*18*) were used in calculating the near-neighbor diagram for Ti_3P-type compounds (Fig. 3). These parameters vary somewhat from one compound to another (see Table 5 in Ref. (*18*)), and it is desirable to know whether the variations can have a serious influence on the resulting diagram. Near-neighbor diagrams were, therefore, constructed using the parameters for the compounds Zr_3P and Nb_3P. These parameters differ from those of Nb_3Si to the greatest extent observed but a comparison of the three diagrams reveals only some relatively minor changes which are, in fact, negligible. It appears justifiable, therefore, to regard these parameters as being fixed at the values reported for Nb_3Si (*18*).

Near-Neighbor Diagrams

"Near-neighbor" diagrams were first proposed by Pearson (*4*) as a way to ana-

[2] For example, Teatum *et al.* (*17*) assign values of 1.390 Å for the atomic radius of As and 1.369 Å for that of Ge, while the *A*15 lattice parameter (extrapolated) for V_3As is 4.744 (see Table I) and 4.780 for V_3Ge. Similarly, the observed *A*15 lattice parameters are 4.621 for Cr_3As and 4.632 for Cr_3Ge. Thus, the observed lattice parameter variations contradict those which would be predicted using the radii of Teatum *et al.* This is not surprising since As and Ge use different bond hybridizations and, hence, have different sizes in different structures.

TABLE I

ATOM SIZE RATIOS (D_B/D_A) AND OBSERVED LATTICE PARAMETER VALUES FOR BINARY A15 COMPOUNDS[a]

System	D_B/D_A	a (Å)
Nb–Si	0.898	5.110[b]
Zr–Au	0.900	5.486
Nb–Rh	0.917	5.130
Nb–Os	0.922	5.135
Nb–Ir	0.924	5.134
V–Ni	0.926	4.680[b]
Ti–Ir	0.929	5.012
V–Co	0.930	4.688
Nb–Ge	0.933	5.135[b]
Mo–Si	0.943	4.893
Nb–Pt	0.945	5.149
Ta–Pt	0.945	5.143[b]
Ti–Pt	0.949	5.032
Nb–Ga	0.962	5.165[b]
Zr–Sn	0.964	5.686[b]
Mo–Os	0.966	4.969
Mo–Ir	0.969	4.970
Mo–Tc	0.972	4.960[b]
Nb–Al	0.976	5.182[b]
Mo–Ge	0.978	4.933
V–Si	0.980	4.724
Zr–Hg	0.982	5.558
Nb–Au	0.982	5.203
Ta–Au	0.983	5.193[b]
Ti–Au	0.986	5.098
Mo–Pt	0.991	4.991[b]
V–Rh	0.999	4.786
V–Os	1.005	4.797[b]
V–As	1.007	4.744[b]
Mo–Ga	1.008	4.933
V–Ir	1.008	4.788
V–Ge	1.017	4.780[b]
Mo–Al	1.023	4.950
V–Pd	1.023	4.826
Cr–Si	1.029	4.556
V–Pt	1.031	4.817
Cr–Ru	1.045	4.677
V–Ga	1.048	4.818
Cr–Rh	1.049	4.674
Nb–Sn	1.053	5.289
Ta–Sn	1.053	5.278[b]
Cr–Os	1.055	4.676
Cr–Ir	1.058	4.682[b]
V–Al	1.064	4.843
Cr–Ge	1.068	4.632
Zr–Tl	1.071	5.725[b]
V–Au	1.072	4.884[b]
Ti–Hg	1.076	5.189
Cr–Pt	1.082	4.674[b]
Nb–Sb	1.083	5.260[b]
Ta–Sb	1.083	5.260
Cr–As	1.085	4.621
Ti–Sb	1.087	5.220
Nb–Te	1.089	5.261
Zr–Pb	1.093	5.659
Cr–Ga	1.100	4.654
Mo–Sn	1.104	5.094
Nb–In	1.133	5.330[b]
V–Sn	1.148	4.995[b]
Nb–Bi	1.157	5.320
Nb–Tl	1.170	5.360[b]
Ti–Tl	1.174	5.360[b]
V–Sb	1.181	4.950[b]
Nb–Pb	1.192	5.370[b]

[a] These values were used in plotting Fig. 2.

[b] Value was corrected for an observed deviation from the ideal A_3B stoichiometry.

lyze a crystal structure by considering the atoms as being compressible rather than rigid. The diagrams are obtained by selecting some arbitrary interatomic distance (such as the closest B–B distances, d_B) for use as a reference in establishing a strain parameter. The known structure geometry permits one to define all of the other interatomic distances relative to d_B. Precise atom contacts are taken to possess zero strain and any atom pair may be placed in precise contact, hypothetically, by letting $d_A = D_A$, $d_B = D_B$, or $d_{AB} = \frac{1}{2}(D_A + D_B)$ depending on the type of atom pair under consideration. D_A and D_B are the atomic diameters of the A and B atoms, respectively, which may be either assumed values or values derived from the structures of the pure elementary components.

One may now evaluate the strains reflected in d_B when contact is established for any other atom pair. The strain parameter is defined by an expression such as (D_B

$- d_B)/D_A$ which can be rewritten as $D_B/D_A - d_B/D_A$. The conditions of close contact, defined above, permit one to evaluate this expression for any distance in the structure since d_B is related to each distance through the structure geometry. Thus, one can evaluate the strain parameter for hypothetical cases as well as for real ones and over a continuous range of values for D_B/D_A. This produces lines in the diagram which indicate predicted strain variations due to atom contacts for a particular distance as a function of the atomic diameter ratio D_B/D_A (see Ref. (*4*)). When the experimental points fall above a given line, it indicates that the observed distance is compressed relative to the respective elementary atomic diameters. Experimental points which fall below the line indicate an expansion of the observed distance. Thus, one can see which of the distances in the structure exert the greatest influence in determining the lattice parameters of the observed compounds having this structure. Near-neighbor diagrams are presented for the *A*15-type compounds in Fig. 2 and for the Ti_3P-type compounds in Fig. 3. Figures 4 and 5 show the distances schematically by presenting the coordination polyhedra around the *B* elements in each structure. These polyhedra include all of the independent distances in the *A*15 structure and all except the shortest *A*–*A* distance in the Ti_3P structure which is treated separately.

Pearson concludes from his near-neighbor diagram for the *A*15 structure that the

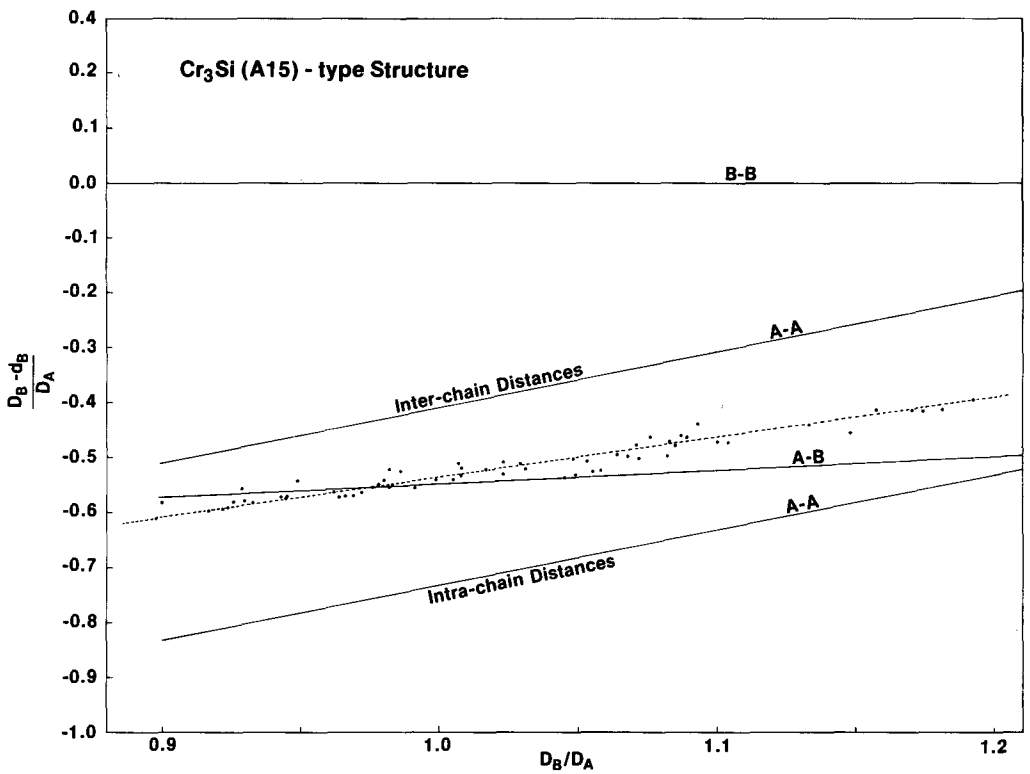

FIG. 2. Near-neighbor diagram for the *A*15-type compounds. The broken line shows the trend of the experimental points for observed compounds. D_A and D_B are the atomic diameters of the *A* and *B* atoms, respectively (see Ref. (*17*)), and d_B is the interatomic distance between the nearest *B* atoms in the structure (see Ref. (*4*)).

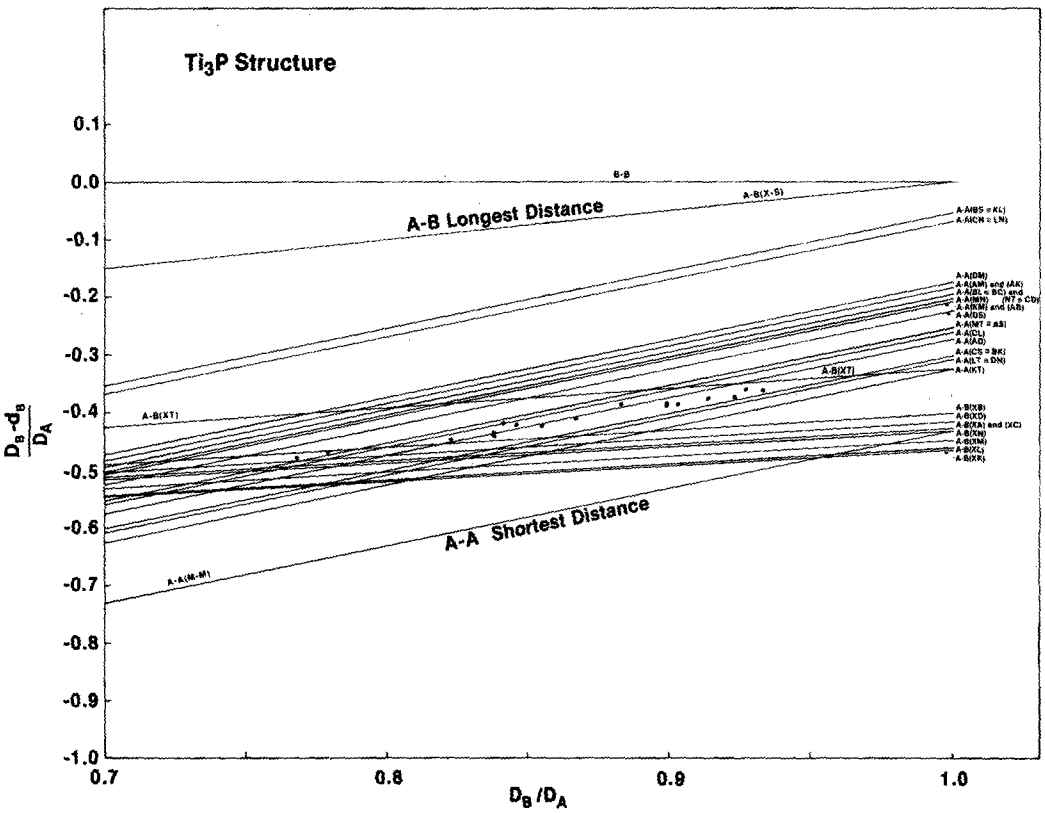

FIG. 3. Near-neighbor diagram for the Ti_3P-type compounds. Black dots are the experimental values for observed compounds. D_A, D_B and d_B are as defined in Fig. 2.

formation of an *A*15-type compound is dominated by a "coordination factor" such that each atom in the structure tries to obtain the maximum number of contacts with its neighbors (*4*). However, the more accurate data, shown in Table I and Fig. 2, indicate that the dominant factor may actually be a "geometric factor." Note that the *A*–*A* intrachain distances are always compressed in this structure while the *A*–*A* interchain distances are always expanded. Note also that the intrachain compression *increases* significantly as the atom size ratio D_B/D_A decreases. It will be shown that this may be an important reason for the instabilities which have been observed in many *A*15 compounds.

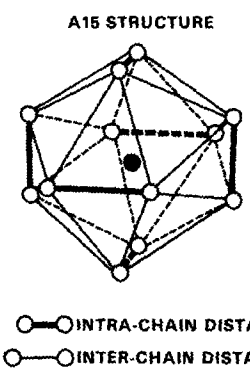

FIG. 4. Identification of the interatomic distances in the *B*-element coordination polyhedron for the *A*15 structure.

The near-neighbor diagram for Ti_3P-type compounds indicates that the "coordination factor" is not very important for these compounds although it could be important

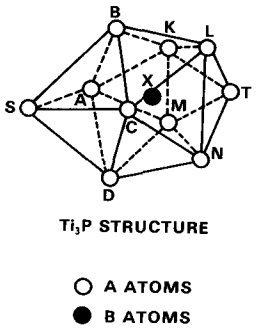

FIG. 5. Identification of the interatomic distances in the *B*-element coordination polyhedron for the Ti_3P structure.

when $D_B/D_A \cong 0.7$. Most of the *A*–*B* distances are slightly compressed while most of the *A*–*A* distances are expanded relative to their respective elementary distances. The formation of these compounds seems to be influenced by a true "geometric factor" similar to that observed by Pearson in the Laves-type phases (*4*). The atoms in such phases tend to be either compressed or expanded in order to obtain the most efficient filling of space. In the Ti_3P phases this usually requires a compression of the *B* atoms and an expansion of the *A* atoms. The absolute magnitude of these distortions, however, cannot be obtained from the near-neighbor diagram since the strain parameter is an arbitrary one. It is noteworthy that the *A*–*A* distances are generally expanded in the Ti_3P structure at atom size ratios where the intrachain distances in an *A*15 structure would be forced into a strong compression. This might account for the increased stability of the Ti_3P structure at atom size ratios approaching $D_B/D_A = 0.9$ where the stability of the *A*15 structure is apparently decreasing. These effects may be further elucidated by a detailed examination of the geometry of these two structures. It is convenient to do this by focusing attention on the *B*-element coordination polyhedra.

B-Element Coordination Polyhedra

Each crystallographic site in a structure is surrounded by a spatial region in which all points are closer to that central site than to any other atom site. Frank and Kasper (*13*) refer to these polyhedral regions as being the "domains" of the central atoms. They define any pair of atoms to be "neighbors" if these atoms share a common domain boundary. This definition is quite rigorous and particularly appropriate for metallic compounds having relatively close-packed structures.

The number of neighbors around the central atom is called its "coordination number" (CN) and when these surrounding "neighbor" sites are connected with straight lines, the lines form the edges of a closed polyhedron known as the "coordination polyhedron" of the central atom (*13*). It is particularly illuminating to examine the *B*-element coordination polyhedra in the *A*15- and Ti_3P-type structures and to note the ways in which they differ from the configuration to be expected if they were composed of rigid spheres.

Idealized *B*-Element Polyhedra

In the following, it is assumed that the atoms of a given *A* element behave as rigid spheres, all of equal size, and that they always remain in contact with neighboring spherical atoms including those of the *B* element. The irregular CN12 atomic configurations around each *B* element in the *A*15 structure must then form perfect regular icosahedra as shown in Fig. 6. An icosahedral configuration of this type composed of rigid spheres requires a central atom diameter at least 10% smaller than the diameter of its surrounding atoms if the surrounding spheres are to remain in contact with each other. All of the *A*–*A* distances are equal. The *A*–*B* distances are shorter than the *A*–*A* distances but are

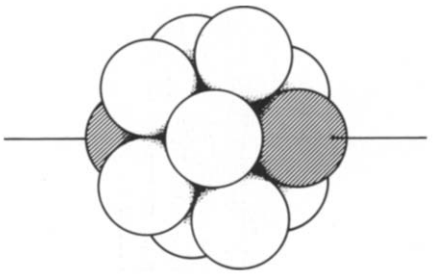

FIG. 6. Idealized rigid-sphere packing for the *B*-element atomic coordination in the *A*15 structure. Shaded spheres show one of the 12 five-fold symmetry axes.

equal to each other. The "ideal" atomic icosahedron, however, cannot be packed with other identical polyhedra to fill space completely and thus form a macroscopic crystal unless some of the atoms are permitted to be nonrigid, nonspherical, or not contacting the others.

The CN 10 atomic configurations around each *B* element in the Ti_3P structure would become dicapped Archimedean antiprisms when composed of rigid contacting spheres (Fig. 7). An atomic configuration of this type requires a central atom diameter at least 36% smaller than the diameter of its surrounding atoms in order to maintain all of its close *A*-atom contacts. The *A*–*A* distances are equal but the *A*–*B* distances comprise two sets. One set of eight *A*–*B* distances is ~18% shorter than the *A*–*A* distances while the other set of two *A*–*B* distances is 13% longer than the *A*–*A* distances. This atomic polyhedron is also difficult (if not impossible) to pack with other identical polyhedra to fill space completely at the A_3B stoichiometry.

It appears, therefore, that the formation of a macroscopic crystal requires that these idealized *B*-element polyhedra be deformed whether they pack with other polyhedra of the same type or with polyhedra of other types which may also impose restrictions on their packing geometry. This has not been proven rigorously, but one may arrive at this conclusion by constructing models. In any case, it is helpful to observe the types of distortions which occur in the *A*15 and Ti_3P structures.

Observed *B*-Element Polyhedra

The observed packing configuration of the *B*-element coordination polyhedra in the *A*15 structure is shown in Fig. 8. The identical *A*–*A* distances of the ideal icosahedron are now replaced by two sets of distances, a set of "interchain distances" and a set of "intrachain distances" which are 23% shorter. The *A*–*B* distances remain equal. They are ~12% larger than the *A*–*A* *intrachain* distances and ~10% shorter than the *A*–*A* *interchain* distances. Thus, it appears that the lattice strains resulting from the observed distortions of an ideal isocahedral configuration are probably dis-

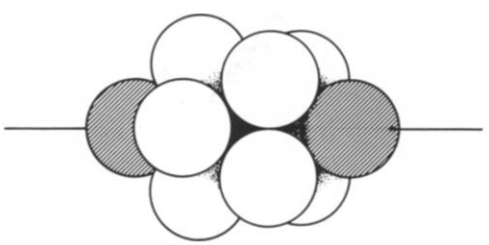

FIG. 7. Idealized rigid-sphere packing for the *B*-element atomic coordination for the Ti_3P structure. Shaded spheres show the single four-fold symmetry axis.

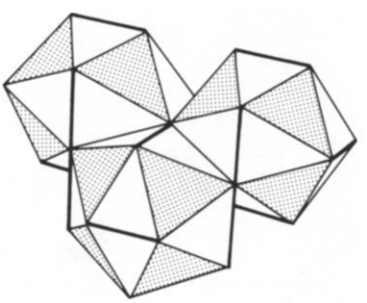

FIG. 8. Packing configuration of the *B*-element coordination polyhedra in the *A*15 structure.

tributed rather uniformly among the available distances.

A list of the known *A*15 compounds and their respective atom size ratios (Table I) reveals that none of these compounds involve a *B* atom which is more than ~10% smaller than its accompanying *A* atom as would be expected if the *A* atoms formed a perfect icosahedron. It is rather remarkable, however, that the *B* atom is sometimes up to 16% *larger* than the *A* atom! This suggests that the *B* atoms in such phases may be "compressed" or, alternatively, that the *A* atoms are either distorted, expanded, or have lost contact with each other.

The observed packing configuration of the *B*-element coordination polyhedra in the Ti_3P structure is shown in Fig. 9. The uniform *A*–*A* distances and the two sets of *A*–*B* distances in the ideal dicapped Archimedean antiprism are now both replaced by a range of unequal distances. These distortions are probably a result of atomic packing requirements since it has been found by experiment that such distortions are necessary if these polyhedra are to pack together in the manner shown in Fig. 9. A noteworthy feature of the observed distortion is that the central *B* atom is located significantly closer to one of the pyramidal end caps than to the other, and this seems to be responsible for a difference in the perimeters of the square bases of these pyramids. In effect, the *B* element seems to be moving toward a smaller coordination number (CN9 instead of the ideal CN10). It is important to point out, however, that the question of whether the CN in these polyhedra are being increased or decreased depends critically in this case on how one arbitrarily defines an atom "neighbor." (See Ref. (*19*).)

If one adopts the Frank–Kasper definition, then the CN is unequivocally 10 since the atomic "domain" (Wigner–Seitz cell) for the *B* atom (assuming the atomic position parameters for Nb_3Si) has 10 faces as shown in Fig. 10. The definition of O'Keefe (*16*) gives a CN of 8.04, however, and other methods yield values between 8 and 9 (14, 15, 19). The 10th atom is located at a significantly greater distance from the central *B* atom than the other 9 neighboring atoms, and the lack of agreement for the various definitions arises largely from differing approaches to the question of how this atom should be treated. The opinion adopted in this paper is that the Frank–Kasper definition (*13*) would probably be

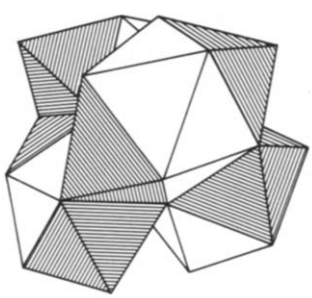

FIG. 9. Packing configuration of the *B*-element coordination polyhedra in the Ti_3P structure. Pyramidal end caps are shaded to show the relative orientation of the polyhedra.

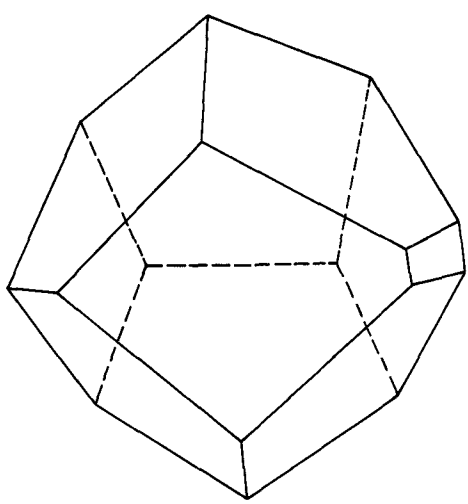

FIG. 10. Wigner–Seitz polyhedron for the *B* atom (Si) in Nb_3Si (Ti_3P-type structure).

most realistic for close-packed metallic compounds of the types being considered.

The list of known Ti_3P compounds and their respective atom size ratios (Table II) shows that none of these compounds has a *B*-atom size which is more than 30% smaller than that of its accompanying *A*-element atom, as would be expected if the *A* atoms formed a perfect cubic antiprism. It is again remarkable that the *B* atom is sometimes much *larger* than the "ideal" size. The *B* atoms seem capable of either expanding their surrounding atom "cages," or, perhaps, themselves undergoing a compression.

It would be interesting to compare the interatomic distances in *A*15 and Ti_3P phases of the same binary system which have the same atom size ratio and are competing for stability. However, these two phases do not coexist in any known binary system. The comparison can be made, however, by using a Nevitt plot (*10*)

TABLE II

ATOM SIZE RATIOS FOR BINARY Ti_3P COMPOUNDS[a]

System	D_B/D_A
Zr–P	0.768
Hf–P	0.778
Zr–Si	0.823
Nb–P	0.838
Ta–P	0.838
Ti–P	0.841
Zr–As	0.846
Zr–Ge	0.855
Hf–Ge	0.867
Y–Sb	0.883
Nb–Si	0.899
Ta–Si	0.899
Ti–Si	0.903
V–P	0.914
Nb–As	0.923
Ti–As	0.927
Ta–Ge	0.933

[a] These values were used in plotting Fig. 3.

to predict the lattice parameters of hypothetical *A*15 compounds and then to compare the calculated interatomic distances with observed distances in the corresponding stable Ti_3P phases such as Nb_3Si, Nb_3As, and Nb_3P (*18, 20*). The results of such a comparison are shown in Table III. In each case the behavior of the interatomic distances is consistent with that to be expected from the analyses based on the near-neighbor diagrams and observed deviations from a "rigid-sphere" model. The average *A*–*B* distance is shorter in the Ti_3P compounds than in the *A*15 compounds. The average *A*–*A* distance in the Ti_3P compounds is significantly larger than the *A*–*A* intrachain distances in the *A*15 structure and are comparable to the *A*–*A* interchain distances. The Ti_3P structure contains one *A*–*A* distance which is comparable to the intrachain *A*–*A* distance in the *A*15 structure but it constitutes only about 6% of the distances and seems to result from atom packing considerations.

Comparison of the *B*-Element Coordination Polyhedra in the *A*15- and Ti_3P-Type Structures

The information obtained from the near-neighbor diagrams and from the observed distortions of the *B*-element coordination polyhedra from a "rigid-sphere" model has identified certain geometric features of the *A*15 and Ti_3P structures which seem to have an important influence on their respective lattice stabilities. It has also shown how the geometry may be affected by variations in the atom size ratios. A critical point seems to be reached when the atom size ratio $D_B/D_A \cong 0.9$ since either the *A*15 or the Ti_3P structure may become unstable at this point. The source of the instability, in the case of the *A*15 phases, seems to be associated primarily with the development of strong repulsive interactions arising from compression of the *A*–*A* intrachain dis-

TABLE III

OBSERVED INTERATOMIC DISTANCES IN Nb-BASED Ti_3P-TYPE COMPOUNDS COMPARED WITH DISTANCES IN THE CORRESPONDING (HYPOTHETICAL) *A*15 COMPOUNDS[a]

Distance[b]	Nb_3As	Nb_3Si	Nb_3P
AB	3.125	3.123	3.100
BC	3.239	3.170	3.175
CD	3.208	3.166	3.140
AD	3.025	2.967	2.931
KL	3.536	3.587	3.527
LN	3.527	3.540	3.405
MN	3.149	3.138	3.100
KM	3.146	3.130	3.061
BK	2.922	2.905	2.903
BL	3.239	3.170	3.175
AK	3.239	3.195	3.182
AM	3.191	3.198	3.154
CL	3.057	3.000	2.946
CN	3.527	3.540	3.405
DM	3.253	3.221	3.189
DN	2.885	2.887	2.833
BS	3.536	3.587	3.527
AS	3.018	3.015	2.966
DS	3.025	3.086	2.999
CS	2.922	2.905	2.903
KT	2.859	2.849	2.819
MT	3.018	3.015	2.966
LT	2.885	2.887	2.833
NT	3.208	3.166	3.140
M–M	2.617	2.644	2.635
XK	2.608	2.578	2.534
XL	2.610	2.586	2.549
XM	2.623	2.608	2.569
XN	2.660	2.637	2.607
XA	2.649	2.651	2.592
XB	2.683	2.701	2.643
XC	2.669	2.642	2.618
XD	2.667	2.667	2.635
XT	2.964	2.857	2.888
XS	3.670	3.778	3.666
Nb–*B* (av)	2.780	2.771	2.730
Nb–Nb (av)	3.156	3.144	3.099
*A*15 compounds			
Predicted *a*(Å)	5.130	5.110	5.070
Nb–*B*	2.873	2.862	2.839
Nb–Nb (interchain)	3.154	3.143	3.118
Nb–Nb (intrachain)	2.565	2.555	2.535

[a] The estimated accuracy is ±0.005 Å.

[b] See Figs. 4 and 5.

tances. There are probably several ways in which one might restore a measure of stability to the structure. One way would be through a deviation from the ideal A_3B stoichiometry in the direction of the larger atom (this is usually an *A* element). This would produce a lattice relaxation which would tend to relieve the internal strains. Another way to produce a relaxation is through the addition of a ternary B-element substitutional solute atom which is larger than the atom which it replaces. Various types of martensitic transformations could also act to relieve the internal strains. Finally, if all else fails, the strains can be very effectively relieved by a transformation to the Ti_3P-type structure. This is accomplished by reducing the atomic coordination of the *B* atom from 12 to 10 which permits a larger *A*-atom spacing and simultaneously permits smaller *A*–*B* distances.

In the case of the Ti_3P phases, instability is associated with a different type of atomic interaction than in the *A*15 phases. The near-neighbor diagram (Fig. 3) indicates that as D_B/D_A approaches 0.9, there is an increasing compression of the *A*–*B* distances in the Ti_3P phases while the *A*–*A* distances remain more or less normal. Thus, the critical destabilizing atomic interaction in the *A*15 structure is the compression of the *A* atoms along the atom chains while, in the Ti_3P structure, the critical interaction is an essentially isotropic compression of the *B* atoms. It should be noted that the *A*–*B* distances in Nb_3As ($D_B/D_A \cong 0.92$) are very close to those in Nb_3Si (Table III) although the atomic (metallic) radius of As is significantly larger than that of Si. One would not expect the *A*–*B* distances to be similar in these two phases unless the As atoms were strongly compressed in Nb_3As.

The geometric effects may or may not be reinforced by electronic "bond" formation, but the existence of electronegativity differences could lead, in certain cases, to partially ionic or partially covalent bonding

which might be compatible with the geometric effects.

Experimental Measurements

It would be most interesting to know whether any of the geometric effects which have been described are reflected in experimental measurements of the physical properties. Strong intrachain repulsive interactions in the *A*15 compounds, for example, should have a detectable effect on the anisotropy of the thermal vibrations for the *A* sites and this anisotropy should, therefore, be greatest when the atom size ratio D_B/D_A approaches the limiting value of 0.9. The available experimental data is insufficient for a complete verification, but it should be noted that measurements on the nonstoichiometric *A*15 phase $Nb_{80}Ge_{20}$ (D_B/D_A = 0.93) have shown that vibrations along the atom chains are 63% as large as those transverse to the chains (*21*). This may be compared with a corresponding value of 71% for the *A*15 compound Nb_3Sn (*22*) which has an atom size ratio D_B/D_A = 1.05. Stoichiometric Nb_3Ge could be expected to show an even greater thermal anisotropy in the atom chain sites than that of $Nb_{80}Ge_{20}$ (i.e., the ratio should be significantly less than 63%) since smaller lattice parameters should produce stronger intrachain repulsive forces. The observed difference in thermal anisotropy for Nb_3Ge and Nb_3Sn might be attributed to differing atomic bonding forces, but Ge and Sn atoms would be unlikely to produce a significantly different bonding in the Nb–Nb atom chains.

Conclusion

The observed interatomic distances in *A*15- and Ti_3P-type compounds have been analyzed as deformations from ideal atomic rigid-sphere behavior. This is accomplished by the use of "near-neighbor diagrams" and by studying the structural geometry of "*B*-element coordination polyhedra." The analysis suggests that structural instabilities develop in *A*15 compounds as the atomic size of the *B* element becomes approximately 10% smaller than that of the *A* element. These instabilities are due to strong repulsive interactions along the directions of the atom chains. It appears that the strains associated with these interactions might be relieved by martensitic transformations or by deviations from ideal A_3B stoichiometry in the "*A*-rich" direction. If this fails to stabilize the structure, one can expect to see a phase transformation. The Ti_3P structure appears to be a favored alternative to the *A*15 structure since it can accommodate smaller *B*-element atoms without producing too many strong repulsive interactions between the *A*-element atoms. This is accomplished by a reduction of the *B*-element coordination from CN12 in the *A*15 structure to CN10 in the Ti_3P structure.

The Ti_3P structure, however, tends to become unstable as the atom size of the *B* element approaches that of the *A* element. The instability, in this case, is due to a strong compression of the *B*-element atom. Thus, the critical interaction in *A*15 phases is an *A*–*A* interaction whereas, in the case of the Ti_3P phases, it is an *A*–*B* interaction (*23*).

The geometric effects may or may not be accompanied by "bond" formation, but partially covalent or partially ionic interactions may be superimposed on the geometric effects as a result of differences in the atomic electronegativities of the component elements. The existence of the geometric effects described here is supported by experimental measurements of the anisotropy of the thermal parameters for certain *A*15 compounds.

Acknowledgment

The author wishes to express his appreciation to

Professors J. Müller and E. Parthé of the Université de Genève for their support and encouragement, as well as for many helpful discussions. He is also indebted to Dr. W. B. Pearson of the University of Waterloo for much valuable advice on the use of near-neighbor diagrams. The Wigner–Seitz polyhedron shown in Fig. 10 was produced using the computer program BLOCKJE written by Dr. Louise Gelato at the Laboratoire de Cristallographie aux Rayons X, Université de Genève, Geneva, Switzerland.

References

1. L. PAULING, "The Nature of the Chemical Bond," 3rd ed., Cornell Univ. Press, Ithaca, N.Y. (1960).
2. Ref. (*1*), pp. 400–401.
3. L. PAULING, *Acta Crystallogr. Sect. B* **24,** 5 (1968).
4. W. B. PEARSON, *Acta Crystallogr. Sect. B* **24,** 1415 (1968).
5. W. B. PEARSON, "The Crystal Chemistry and Physics of Metals and Alloys," p. 52, Wiley–Interscience, New York (1972).
6. R. M. WATERSTRAT, F. HAENSSLER, AND J. MÜLLER, *J. Appl. Phys.* **50,** 4763 (1979).
7. G. R. JOHNSON AND D. H. DOUGLASS, *J. Low-Temp. Phys.* **14,** 575 (1974).
8. W. B. PEARSON, "The Crystal Chemistry and Physics of Metals and Alloys," p. 24, Wiley–Interscience, New York (1972).
9. G. GELLER, *Acta Crystallogr.* **9,** 885 (1956).
10. M. V. NEVITT, "Electronic Structure and Alloy Chemistry of the Transition Elements" (P. A. Beck, Ed.), p. 123, Interscience, New York (1963).
11. J.-L. STAUDENMANN, *Solid State Commun.* **23,** 121 (1977).
12. J.-L. STAUDENMANN, P. COPPENS, AND J. MÜLLER, *Solid State Commun.* **19,** 29 (1976).
13. F. C. FRANK AND J. S. KASPER, *Acta Crystallogr.* **11,** 184 (1958).
14. G. O. BRUNNER, *Acta Crystallogr. Sect. A* **33,** 226 (1977).
15. F. L. CARTER, *Acta Crystallogr. Sect. B* **34,** 2962 (1978).
16. M. O'KEEFE, *Acta Crystallogr. Sect. A* **35,** 772 (1979).
17. W. B. PEARSON, "The Crystal Chemistry and Physics of Metals and Alloys," p. 151, Wiley–Interscience, New York (1972).
18. R. M. WATERSTRAT, K. YVON, H. D. FLACK, AND E. PARTHÉ, *Acta Crystallogr. Sect. B* **31,** 2765 (1975).
19. S. RUNDQVIST, Y. ANDERSON, AND S. PRAMATUS, *J. Solid State Chem.* **28,** 41 (1979).
20. P. NAWAPONG, *Acta Chem. Scand.* **20,** 2737 (1966).
21. S. E. RASMUSSEN AND R. G. HAZELL, *Acta Crystallogr. Sect. B* **35,** 1677 (1979).
22. B. N. KODESS, *Phys. Lett. A* **73,** 53 (1979).
23. R. M. WATERSTRAT, *J. Less-Common Metals* **43,** 105 (1975).